Hippocampal Neuropeptide Y_2 receptor blockade improves spatial memory retrieval and modulates limbic brain metabolism

Running Title: NPY Y_2R modulates brain metabolism and spatial memory

Marta Méndez-Couz [a,b*], Héctor González-Pardo [a,c], Jorge L. Arias [a,c], Nélida M. Conejo [a,c]

a- Laboratory of Neuroscience, Department of Psychology, Instituto de Neurociencias del Principado de Asturias (INEUROPA), University of Oviedo, Pl. Feijoo s/n. 33003, Oviedo (Spain).

b- Dept. Neurophysiology. Medical Faculty. Ruhr-University Bochum. Universitätsstraße 150. Building MA 4/158. 44780 Bochum (Germany)

c- Instituto de Investigación Sanitaria del Principado de Asturias (ISPA), 33006 Oviedo, Spain.

***Correspondence:** Marta Méndez-Couz. Dept. Neurophysiology. Medical Faculty. Ruhr-University Bochum. Building MA 01/551. Universitaetsstraße 150, 44780. Bochum (Germany). Phone: ++49 - (0)234 - 32 – 27927. Email: marta.mendezlopez@rub.de

Highlights:

- Under hippocampal Y_2R antagonism, place preference memory retrieval is enhanced
- Spatial retrieval enhancement under Y_2R blockade is correlated with changes in regional brain energy metabolism
- Enhanced retrieval associated CCO activity increases in the dorsal DG, while decreasing in the ventral CA1, IL cortex and mammillary bodies
- Y_2R exert control over patterns of brain activation that are relevant for spatial memory expression

ABSTRACT

Introduction: The neuropeptide Y (NPY) is broadly distributed in the central nervous system (CNS), and it has been related to neuroprotective functions. NPY seems to be an important component to counteract brain damage and cognitive impairment mediated by drugs of abuse and neurodegenerative diseases, and both NPY and its Y_2 receptor (Y_2R) are highly expressed in the hippocampus, critical for learning and memory. We have recently demonstrated its influence on cognitive functions; however, the specific mechanism and involved brain regions where NPY modulates spatial memory by acting on Y_2R remain unclear. **Methods:** Here, we examined the involvement of the hippocampal NPY Y_2R in spatial memory and associated changes in brain metabolism by bilateral administration of the selective antagonist BIIE0246 into the rat dorsal hippocampus. To further evaluate the relationship between memory functions and neuronal activity, we analysed the regional expression of the mitochondrial enzyme cytochrome c oxidase (CCO) as an index of oxidative metabolic capacity in limbic and non-limbic brain regions. **Results:** The acute blockade of NPY Y_2R significantly improved spatial memory recall in rats trained in the Morris water maze that matched metabolic activity changes in spatial memory processing regions. Specifically, CCO activity changes were found in the dentate gyrus of the dorsal hippocampus and CA1 subfield of the ventral hippocampus, the infralimbic region of the PFC and the mammillary bodies. **Conclusions:** These findings suggest that the NPY hippocampal system, through its Y_2R receptor, influences spatial memory recall (retrieval) and exerts control over patterns of brain activation that are relevant for associative learning, probably mediated by Y_2R modulation of long-term potentiation and long-term depression.

Keywords: Dentate Gyrus, infralimbic cortex, cytochrome C oxidase, mammillary bodies, ventral hippocampus, synaptic plasticity

1. INTRODUCTION

Neuropeptide Y (NPY) was isolated and characterized three decades ago (Tatemoto, 1982). This neuropeptide is widely distributed in the central nervous system (CNS), and it has been associated with functions as food intake (Balasubramanian et al., 2021; Comeras et al., 2019; Stanley & Leibowitz, 1984), cognitive processes (Bertocchi et al., 2021; Thorsell et al., 2000), neuroprotection (Malva et al., 2012; Silva et al., 2005), drug addiction (Gonçalves et al., 2016) and regulation of stress, anxiety, and resilience [For a review, see Reichmann and Holzer (2016)]. However, the role of NPY as a memory modulator is still controversial (Gøtzsche & Woldbye, 2016). Previous research showed that the NPYergic system participates in cognitive processes either improving or impairing short- and long-term memory, and these effects are claimed to be both dose- and brain region-specific (Bertocchi et al., 2021; Flood et al., 1987; Gøtzsche & Woldbye, 2016; Kornhuber & Zoicas, 2017, 2020; Thomas & Ahlers, 1991).

The CNS NPYergic system exerts its effects through Y_1-Y_6 receptors (Parker & Herzog, 1999; Xapelli et al., 2006). All of them are postsynaptic receptors, except Y_2R, a presynaptic autoreceptor that inhibits NPY release (Decressac & Barker, 2012; Stanić et al., 2006; Stanić et al., 2011). The hippocampal Y_2R, which presynaptically inhibits glutamate release, also undergoes *de novo* expression in mossy fibres and granule cells (Furtinger et al., 2001; Gobbi et al., 1998).

NPY and its receptors are highly expressed in brain regions that contribute to cognitive processing (Parker & Herzog, 1998, 1999). Specifically, Y_2R is highly expressed in the amygdala, hippocampus and hypothalamus, the brain areas considered essential for contextual memory processes, and their integration with emotional components (Stanić et al.,

2011). In the hippocampus, Y_2R is found at higher levels in the pyramidal cell layers of CA1 and CA3, although is also present in the DG-hilus region(Parker & Herzog, 1999).

Regarding the specific effects of the NPYergic system on learning and memory, a growing body of literature suggests its involvement in the encoding and recall learning phases (Bertocchi et al., 2021; dos Santos et al., 2013; Hörmer et al., 2018; Méndez-Couz et al., 2021). Interestingly, NPY showed a neuroprotective role against methamphetamine-induced excitotoxicity in the hippocampus (Gonçalves et al., 2012) or against oxidative stress, via Y_2R, preventing depressive behaviour and spatial memory deficits in mice (dos Santos et al., 2013).

For cognitive processing to occur, neurons carry on multiple energy-consuming activities (Wong-Riley, 1989, 2012). Their supply of energy, in form of ATP, comes almost entirely from oxidative phosphorylation, in contrast to astrocytes that rely on glycolysis (Almeida et al., 2004), which make them heavily dependent on mitochondrial function. The brain metabolic state was analysed in this study using a cytochrome c oxidase (CCO) activity analysis. CCO is the last member of the electron transport chain located in the inner mitochondrial membrane [see review by Chicherin et al. (2019)]. The tight coupling between neuronal activity and oxidative energy metabolism converts the CCO activity into a good and useful endogenous metabolic biomarker for neuronal activity (Gonzalez-Lima & Cada, 1994; Gonzalez-Lima & Jones, 1994; Wong-Riley, 1989, 2012). CCO activity can, therefore, be interpreted as a history of cumulative energy demands of brain cells underlying prolonged stimulation or training on behavioural tasks – days or weeks – (Agin et al., 2001; Bertoni-Freddari et al., 2001; Conejo et al., 2010; Hescham et al., 2014); this represents a complementary technique to the more short-lived immediate early genes (IEG) studies (minutes or several hours after evoked neuronal stimulation). CCO quantitative histochemistry has also proved to be a reliable method to measure changes in brain

metabolism associated with endocrine alterations and neurodegeneration (Morán et al., 2013) as well as learning and memory processing (Conejo et al., 2010; Gasalla et al., 2016; Méndez-Couz et al., 2016) and, specifically, to measure brain regional changes associated with the retrieval of spatial learning (Conejo et al., 2013; Méndez-Couz et al., 2015a; Zorzo et al., 2021a; 2021b).

Following the stimulation of N-Methyl-D-aspartate (NMDA) receptors, neurons transiently synthesize nitric oxide (NO) in a calcium/calmodulin -dependent manner. NPY modulates the production of NO in the microglia induced by interleukin-1β (IL-1β). As shown by other authors (Ferreira et al., 2010; Malva et al., 2012), NPY treatment inhibits NO production as well as the expression of inducible nitric oxide synthase. Nitric oxide acts as a cellular messenger, activating soluble guanylyl cyclase and participating in the transduction signallin g pathways involving cyclic GMP [See (Moncada & Bolaños, 2006)]. NO production can also act as a pathophysiological mediator, related to heart failure among other diseases (Almeida et al., 2004; Moncada & Bolaños, 2006). In the CNS, high amounts of NO inhibit the mitochondrial CCO in neurons, resulting in neuronal depolarization and calcium-dependent vesicular glutamate release, followed by excitotoxicity. Ultimately, neurons die by excitotoxicity via NMDA (Brown, 2007). NO also binds to CCO, inhibiting cell respiration in a reversible process, competing with oxygen (Moncada & Bolanos, 2006) and leading to the release of superoxide anion from the respiratory chain. Besides, NPY is a known regulator of feeding and energy metabolism by affecting mitochondria that, in turn, act as energy sensors in AgRP/NPY hypothalamic neurons. This stimulates appetite and increases energy oxidative metabolism (Billington & Levine, 1992; Haigh et al., 2020; Su et al., 2016). Therefore, NPY can ultimately modulate the activity of key mitochondrial enzymes involved in cellular respiration and oxidative metabolism like CCO, measured here.

In a previous NPY receptor expression study, we showed changes in spatial memory task performed under serial Y_2R blockade (Méndez-Couz et al., 2021), associated with NPY Y_1R and Y_2R brain expression changes in the dorsal hippocampus and the prefrontal cortex, suggesting a rapid metaplastic regulation of NPY receptors contributing to spatial memory. The specific role of NPY via Y_2R on spatial orientation memory, including the region-specific involvement and its mechanism of action in this process, remains – nevertheless – unknown.

In the current study, we evaluated the brain regional metabolic activity changes following a spatial memory recall task under acute infusion of a Y_2R intrahippocampal antagonist, which improved spatial memory associated with the increased metabolic activity of the DG, and decreased metabolic activity in the CA1 subfield of the ventral hippocampus, the infralimbic cortex and mammillary bodies.

2. MATERIAL AND METHODS

2.1. Animals

Male adult Wistar rats (*Rattus norvegicus)*, weighing between 250–330g, were used (N=30). They were obtained from the University of Seville central animal facilities (Seville, Spain) and housed in a temperature-controlled room (23±2ºC). Lighting was kept on a 12-h light/dark cycle with lights on from 08:00–20:00 h. Rats were kept in standard laboratory cages (20 × 35 × 55 cm), with four rats in each cage with *ad libitum* access to food and tap water.

2.2 Behavioural procedure

The rats were first tested in a neurological assessment battery to discard possible motor and sensory deficits before and after the surgery. The neurological tests used allowed us to evaluate the following reflexes: abduction response of hind limbs, grasping reflex, extension and flexion reflexes, hearing and vestibular responses, head shaking reflex, pupillary reflex,

147 negative geotactic responses and righting reflex (Bures et al., 1976). Rats were handled daily,
148 5 days before the surgery, to reduce anxiety-like behaviour related to contact with the
149 experimenters. See the timeline of the experiment in Figure 1.

150 **2.3. Surgery**

151 Rodents were deeply anaesthetized with xylazine (5 mg/kg, i.m.) and ketamine (80-100
152 mg/kg, i.p.), and set in a David Kopf (Tujunga, CA) or Narishige (Japan) stereotaxic frame.
153 Stainless steel cannulae of 22G inner diameter (Becton Dickinson S.A., Spain) were
154 stereotactically implanted bilaterally in the CA1 region of the dorsal hippocampus
155 (coordinates from bregma: AP -3.6, L ±2.6, DV -2.1 mm). Cannulae were fixed to the skull
156 using dental acrylic cement (Glaslonomer Cement, Shofu Inc., UK) and anchor screws. Rats
157 were allowed to recover after surgery for 5 days.

158 After this resting period, the rats underwent the same neurological assessment battery
159 explained above to discard any possible abnormality caused by the stereotaxic procedure.

160 **2.4. Groups**

161 Rats were randomly assigned to one of the three experimental groups as follows:
162 1-Control cage (CC): rats maintained in their home cage without further pharmacological,
163 surgical or behavioural interventions. This group was added to ensure that brain metabolic
164 activity changes were due to behavioural and pharmacological modifications.
165 2- Experimental group (Exp): received 1 nmoL/µL BIIE0246 in 0.9% physiological saline
166 containing 1% DMSO (1 µL/hemisphere).
167 3-Control saline vehicle group (Veh): rats were administered 0.9% physiological saline
168 containing 1% DMSO (1 µL/hemisphere).

2.5. Injection

Following the protocol described by Méndez-Couz et al. (2021), rodents received the treatment through the permanent cannula 30 min before the retrieval test was performed on the third day of the Morris water maze (MWM). Rats were randomly assigned to the experimental or vehicle saline group. Solutions were infused at 0.5 µl/min and the microcannula was held inside for an additional 60 s to prevent fluid from backing up into it.

2.6. Spatial memory training

2.6.1. Apparatus

The MWM was composed of a circular water tank made of black fibreglass, measuring 1.5 m in diameter by 75 cm in height (Morris, 1984). Following the experimental setting conditions described by Méndez-Couz et al. (2014,2015a), the pool was filled with tap water, and a black escape platform was placed hidden beneath the water surface. The water temperature was kept at 20±1°C during the entire training period. The pool was surrounded by black panels located 40 cm from the maze, on which highly contrasted printed geometric visual cues were placed, acting as allocentric cues. The room was softly illuminated by two halogen spotlights facing the ceiling (500 W). Each trial was recorded and later analysed offline, using a computerized video-tracking system (Ethovision Pro, Noldus Information Technologies, Wageningen, The Netherlands). Measured variables included the time spent to reach the platform (latencies) when the platform was present in the maze and the time spent in each of the four virtual quadrants in which the pool was divided (A, B, C or target, and D) during the transfer tests.

The behavioural protocol in the water maze was applied as described in Méndez-Couz et al. (2021); it is also briefly detailed below (Figure 1).

192 ### 2.6.2. Pretraining

193 In order to habituate the rats to the task in the MWM, they received a pretraining session with
194 a visible platform present at the centre of the maze. During this first stage, rats received four
195 trials, in which they were released facing the pool walls following a pseudo-random
196 sequence. The escape platform was set 2 cm above the water surface so that it was visible
197 from afar. Rats could swim up to 60 s to locate the platform in each trial or were gently
198 manually guided to it after that time. Once on the platform, rats were left 15 s on it, and they
199 rested 5 s outside the maze in a plastic container until commencing the next trial.

200 ### 2.6.3. Spatial reference memory task: training session

201 During training, the rats were required to locate a hidden platform placed in the centre of a
202 determined quadrant for each rat. Therefore, they had to use external visual cues situated
203 around the pool to perform the task (see Figure 1).

204 After pretraining, on the first day, rats received four training sessions of four trials each,
205 resting 30 min in their home cage between sessions. In each trial, rats were released from the
206 border of each of the quadrants in a pseudorandom order to search for the hidden escape
207 platform located 1.5 cm beneath the water surface (Figure 1, Bottom). Rats were allowed to
208 swim for 60 s to reach the platform or manually guided to it after this time; once they
209 achieved the platform, they remained there for 15 s. The intertrial time was 5 s, in which they
210 were allowed to rest outside the maze in a plastic container, different from their home cage.
211 On the following day, they received three identical sessions of four trials, until accomplishing
212 on average a learning criterion of 20 s latency to reach the platform; training was stopped at
213 this point to avoid overtraining.

214 After the last trial on day two, rats were submitted to a retention probe test trial to find out
215 whether they remembered the location of the hidden platform. During this probe, the platform

was removed from the pool, and rats were released from the contralateral side to the previously reinforced quadrant. The test lasted for 60 s, after which the rats were placed again in a plastic bucket outside the maze. To prevent the early extinction of the previously learned task, all rats received an additional trial in which the platform was present in the maze in its original place. The latencies during this trial were included for analysis together with the data from the last session of acquisition (Figure 2a).

2.6.4. Retrieval test

The day after finishing the second day of acquisition, a retrieval test was performed. Rodents were intracerebrally infused with the drug (1 nmoL/µL BIIE0246 in 0.9% physiological saline + 1% DMSO) or vehicle saline solution 1% DMSO, 30 min before the spatial memory test in the MWM, consisting of four trials in the same conditions as explained above. Additionally, a new memory retention probe test was performed on day three.

2.7. Molecular analysis

2.7.1. Infusion site

All animal brains from the experimental and vehicle groups were analysed for the infusion site through serial brain slices section selection and posterior analysis after cresyl violet Nissl staining according to Paxinos and Watson (2004). One animal was discarded due to injection misplacement. The extension of the drug area of influence at the injection site was estimated in previous pilot studies to be around 1.5 mm in diameter, sufficient to cover the targeted CA1 dorsal field of the hippocampus.

2.7.2. Brain cytochrome c oxidase histochemistry

Randomly selected rats from the vehicle and experimental groups, and additional rats selected as CC group (Veh N=6, Exp N=8, CC N=8) were sacrificed 90 min after finishing the behavioural tasks or directly from the cages in the latter case; brains were quickly

240 removed then frozen in isopentane at -70°C (Sigma–Aldrich, Madrid, Spain) and stored at -
241 40°C, to preserve the brain tissue and enzyme activity. Brains were subsequently cut at 30
242 µm-thick coronal sections using a cryostat microtome (Microm International GmbH, model
243 HM 505-E, Heidelberg, Germany). These sections were mounted on gelatinized slides and
244 stored at -40°C until further processing.

245 A modified version of the quantitative CCO histochemical method developed by Gonzalez-
246 Lima and Jones (1994) was used. Staining variability across different baths was controlled by
247 sets of tissue standards. These standards were obtained from Wistar rat brain homogenates of
248 known CCO activity that were determined spectrophotometrically at different thicknesses
249 (10, 30, 50 and 70 µm). Following the previously described protocol by Conejo et al. (2013),
250 the standards were included with each batch of slides. In short, each set of slides were fixed
251 for 5 min with a 0.5 (v/v) glutaraldehyde solution, rinsed three times in phosphate buffer (PB)
252 and preincubated 5 min in a solution containing 0.05 M Tris buffer pH 7.6 with 275 mg/L
253 cobalt chloride 10% (w/v), sucrose and 0.5 (v/v) dimethylsulfoxide. After the sections had
254 been rinsed in PB (pH 7.6; 0.1 M), they were incubated at 37°C for 1 h in darkness, in a
255 solution containing 50 mg 3,3′-diaminobenzidine, 15 mg cytochrome c (Sigma, St. Louis,
256 MO, USA) and 4 g sucrose per 100 mL PB (pH 7.4; 0.1 M). The reaction was stopped by
257 fixing the tissue in buffered formalin (10% w/v sucrose and 4% formalin) for 30 min at room
258 temperature (RT). After being fixed the slides were dehydrated, cleared with xylene and
259 coverslipped with Entellan (Merck, Darmstadt, Germany).

260 CCO histochemical staining intensity was measured by densitometric analysis using a
261 computer-assisted image analysis workstation and image analysis software (MCID,
262 InterFocus Imaging Ltd., Linton, England). Twelve measurements of relative optical density
263 were taken per region (4 per slice). To compare and consider possible staining variations
264 across brain sections from different staining baths, measurements were also taken from CCO-

stained brain homogenate standards. Regression curves between section thickness and known CCO activity, previously assessed by spectrophotometric assay in each set of standards, were calculated. Lastly, the average relative optical density measured in each brain region was converted into CCO activity units (1 unit: 1 µmol of cytochrome c oxidized/min/g tissue wet weight at 23°C), using the previously calculated regression curve in each homogenate standard. Averages were calculated per region and animal. Regions to analyse included the prelimbic (PL), and infralimbic regions (IL) of the medial prefrontal cortex and primary motor cortex (M1), all of them measured at $^{+}/_{-}$ 3.70 mm from Bregma and the parietal cortex (PAR) $^{+}/_{-}$ -3.80 mm. In addition, the following subcortical regions were also taken: dorsal subfields of hippocampus including CA1, CA3 and dentate gyrus (dCA1, dCA3, dDG) at $^{+}/_{-}$ -3.30 mm and ventral hippocampus subfields (vCA1, vCA3, vDG), taken at $^{+}/_{-}$ -4.52 mm from Bregma. Medial (MeA), basal (BaA), lateral (LaA) and central (CeA) amygdaloid nuclei measured at $^{+}/_{-}$ -3.14 mm from Bregma; medial (MM), lateral (LM) and supramammillary (SuM) nuclei of the mammillary bodies measured at $^{+}/_{-}$ -4.52 mm, as well as the premammillary nucleus (PM) taken at $^{+}/_{-}$ -4.16 mm. The selected brains regions were defined according to Paxinos and Watson's (2004) atlas.

2.8. Statistical analysis

2.8.1. Behavioural tests

A one-way ANOVA test was applied to evaluate the latencies across training sessions during the acquisition days, with "session" as a factor. Two-way repeated-measures ANOVA tests were applied to evaluate the group differences in the escape latencies after the treatment. Afterwards, Holm-Sidak tests were used to further analyse significant interactions between group and training sessions. Holm-Sidak's post-hoc tests were also used to evaluate differences across training sessions in each experimental group. To analyse the swimming time spent in each virtual quadrant of the maze during the retention probe after the

acquisition, a one-way repeated-measures ANOVA was carried out. After the infusion, a two-way RM ANOVA test was used to study these differences in quadrant preference in both experimental groups during the retention probe. Holm-Sidak's post-hoc tests were used in case of significant ANOVA results.

2.8.2. Cytochrome c oxidase histochemistry measurement

Experimental, vehicle saline and CC groups differences in CCO activity measured in each brain region were analysed by a mixed model one-way ANOVA. Tukey's post hoc tests were used to assess differences between pairs of experimental groups when ANOVA indicated significant group differences. Significance levels were set to $p<0.05$. Statistical analysis was performed using Sigma-Plot 11 (Systat Software, Chicago, USA).

3. RESULTS

3.1. Behavioural tests

No rats were discarded due to their neurological reflexes' responses after the surgical procedure.

3.1.1. Rats acquired the hidden platform spatial memory task

Results showed that rats (N=28) acquired the spatial memory task before treatment, as shown by the significant decrease in the latencies needed to reach the platform through the acquisition sessions one to seven ($F_{(6,182)}=10.35$, $p<0.001$). Specifically, the post-hoc test showed differences between the first and the last acquisition session (Holm-Sidak, $p<0.001$) (Figure 2a). By the end of the second day, rats reached, on average, the learning criterion of 20 s to arrive at the platform, so the acquisition phase was considered finished. Rats that failed to reduce the amount of time needed to reach the platform from the first to the last sessions or presented an inverted learning curve were discarded, and their data were not

included in the study (N=2). The acquisition phase was stopped at this point to avoid overtraining, lack of motivation and an early extinction of the previously learned response.

After finishing the acquisition phase, rats underwent a retention probe test, in which a preference for the previously reinforced quadrant was observed ($F_{3,108}$=41.41, p<0.001), (Holm-Sidak between reinforced quadrant and rest of the quadrants, p<0.001) (Figure 3a).

3.1.2. Administration of the Y_2R antagonist improved spatial orientation ability in the MWM test

Rats that had learned the task were randomly assigned to the vehicle or experimental groups. One day after the last acquisition session, they were administered with the saline vehicle or the antagonist solution, respectively, and after 30 min, they were submitted to an early retrieval test consistent in four trials in the MWM. When comparing the latencies to reach the platform through the four post-treatment trials, we found significant differences between vehicle and experimental groups (Two ways RM ANOVA $F_{(1,76)}$=13.58, p=0.001). These differences depended on the analysed trial (Two ways RM ANOVA $F_{(23,76)}$=3.37, p=0.023). Specifically, the vehicle group was slower to reach the platform as compared to the experimental group during the first trial after the drug administration (Holm-Sidak, p=0.001). Eventually, all groups showed improvement, by gradually decreasing latencies to reach the platform over the 4 trials of the test (Trial 8.1 vs Trial 8.4, p<0,001). Both groups needed under 20 s on average to reach the platform in the last trial post-treatment (Figure 2a).

The Y_2R antagonist effect on memory retrieval was also observed in the preference for the reinforced quadrant during the retention probe carried out on the test day. Results show an interaction between group and quadrant factors ($F_{(3,78)}$=4.28; p=0.008). Vehicle and experimental groups spent a significantly different amount of time in the different quadrants of the maze on the test day ($F_{(1,108)}$=5.62; p=0.025). The analysis also showed differences in

the factor quadrant ($F_{(3,98)}$=13.93; p<0.001). Specifically, the experimental group preferred the previously reinforced quadrant on the test day over all other quadrants (Holm-Sidak, p<0.001). Within the vehicle group, the quadrant preference was not so striking, although they spent a higher amount of time in the reinforced quadrant as compared to the lateral quadrant A (p=0.009) and the contralateral D (p=0.033), but not to the other lateral quadrant B (p=0.38). When the amount of time swimming in the reinforced quadrant was compared between both groups, this result was confirmed, as the experimental rats spent more time searching in the previously reinforced quadrant than the vehicle rats (t=3.11, p=0.02) (Figure 3b).

3.2. Metabolic activity increased in the dorsal DG and decreased in the ventral Ca1, IL cortex and mammillary bodies following spatial training under NPY Y_2R blockade

Significant group differences in CCO activity were found in the prelimbic cortex ($F_{(2,21)}$= 8.57; p=0.002), infralimbic cortex ($F_{(2,21)}$=8.68; p=0.002), parietal cortex ($F_{(2,19)}$= 8.68; p=0.002), CA1 region ($F_{(2,20)}$= 4.67; p=0.023) and dentate gyrus ($F_{(2,20)}$= 4.93; p=0.02) of the dorsal hippocampus. Additionally, statistical differences were found in the CA1 region of the ventral hippocampus ($F_{(2,21)}$= 5.78; p=0.01), the central ($F_{(2,19)=}$ 26.88; p<0.001) and lateral ($F_{(2,19)}$= 3.81; p<0.05) nuclei of the amygdaloidal complex and the medial mammillary nucleus ($F_{(2,17)}$= 12,45; p<0.001). Figure 4a, Figure 4b and Table 1 show the mean CCO activity values measured in the regions of interest of the different experimental groups, including a control cage (CC) group, used as a baseline for comparison.

In particular, Tukey's HSD tests showed significant increases in CCO between groups trained in the water maze (Exp-Veh) as compared to the CC group; specifically, the activity of the prelimbic cortex was higher in Veh (p=0.021) and Exp (p=0.003) groups as compared to the CC group. In contrast, CCO activity was lower in the Veh and Exp groups in the

central nucleus of the amygdaloid complex (p<0.001) as compared to the CC group. A similar effect was found in the lateral nucleus of the amygdaloid complex (p<0.001) in between the Exp and the CC group. Finally, the CA1 region of the dorsal hippocampus presented higher CCO activity in the CC group as compared to the Veh group (p=0.02).

On the other hand, the effect of the drug was observable in the differences found between Exp and Veh groups; specifically, significantly lower CCO activity was detected in the Exp group infralimbic region of the mPFC and the parietal cortex (p=0.002) (figures 4a and 4c). Additionally, significantly higher CCO activity (p=0.05) was found in the dentate gyrus of the dorsal hippocampus in the Exp group (figures 4a and 4d), whereas the ventral CA1 CCO activity was lower in the Exp than in the rest of the groups (figures 4b and 4f). Lastly, the mammillary nucleus of the Exp group showed significantly lower CCO activity (p<0.001) as compared to the rest of the groups (figures 4b and 4e).

4. DISCUSSION

The results of this study show that hippocampal NPY Y_2R antagonism enhances spatial memory retrieval and alters retrieval-induced brain metabolic activity. Following retrieval under Y_2R blockade, increased metabolic activity was detected in the DG of the dorsal hippocampus, and decreased activity was detected in the ventral CA1 hippocampal subfield, the medial mammillary bodies and the infralimbic region of the mPFC. Our findings support the notion that the NPY system is involved in spatial memory through the activation of Y2 receptors. Moreover, it suggests that Y_2R-dependent changes in metabolic activity are a mechanism involved in spatial memory processing.

4.1. Intrahippocampal administration of an NPY Y_2R antagonist rapidly improves the early recall of spatial reference memory

To evaluate the mnemonic effects of the NPY system in cognition, we used a hidden platform task in the MWM paradigm (Morris, 1984), the most used paradigm to study, in rodents, spatial memory, that is heavily dependent on intact hippocampal function (Méndez-Couz et al., 2015a; Méndez-Couz et al., 2015b; Zorzo et al., 2021a).

All groups of rats displayed similar decreasing latencies to reach the platform along training days and a preference for the previously reinforced virtual quadrant on the retention probe, showing that rats successfully acquired the initial spatial memory.

However, rats receiving intrahippocampal infusions of the Y_2R antagonist performed better than those in the vehicle group, presenting lower latencies to reach the escape platform and more time spent in the reinforced quadrant during the retention probe. The results are consistent with differential sub-acute and acute effects of hippocampal NPY in the cognitive processes involved in the spatial reference memory task (Méndez-Couz et al., 2021). Likewise, other studies applying acute infusions of Y_2R antagonists in the lateral ventricles (Kornhuber & Zoicas, 2017), dorsal hippocampus, amygdala or dorsolateral septum (Kornhuber & Zoicas, 2020) reported both Y1 and Y2 receptor-mediated NPY neurotransmission as necessary for retention and retrieval of hippocampus-dependent tasks, such as object recognition and retrieval of social memory. Together with our results, this would suggest the region-specific and memory type-specific role of NPY acting on Y1 or Y2 receptors on distinct phases of memory.

The NPY system is well known to be related to anxiety and mood regulation (Gøtzsche & Woldbye, 2016; Nwokafor et al., 2020; Thorsell et al., 2000; Vázquez-León, Ramirez-San Juan, Marichal-Cancino, Campos-Rodriguez, Chavez-Reyes, and Miranda-Paez et al., 2020).

On the other hand, the role of Y_2Rs in spatial versus emotional learning is still controversial (Hörmer et al., 2018; Tasan et al., 2016). In this regard, stress and locomotor activity could have affected the performance in the MWM test. In previous studies with this model (Méndez-Couz et al., 2021), we found, however, no anxiogenic or anxiolytic behavioural effects, ruling out the exclusively stress-related treatment influence on the subsequent MWM task. Additionally, previous studies in knockout Y_2R (-/-) mice failed to show alterations in locomotor activity (Redrobe et al., 2004; Tschenett et al., 2003) or anxiety-related behaviour (Zambello et al., 2011). More recently, Hörmer et al. (2018) reported that the hippocampal Y_2Rs modulate memory depending on its emotional valence, enhancing spatial memory while delaying fear conditioning memories. Taken together, these results suggest that the NPY Y_2R blockade induced mnemonic-associated functional changes that are not exclusively attributable to anxiolytic or anxiogenic effects of the drug. Therefore, the observed regional metabolic changes (see below) are likely to be related to the specific effects of the treatment on retrieval of spatial memory.

4.2. Hippocampal NPY Y_2R blockade before spatial memory retrieval changes metabolic activity in the dorso-ventral hippocampus, infralimbic cortex and mammillary bodies

The dynamic changes in brain metabolism in the dorsal and ventral hippocampus, mammillary bodies and prefrontal cortex after Y_2R antagonist treatment were striking and may serve to explain the observed effects on behavioural performance.

We found a generalized reduction of CCO activity in the experimental group after retrieval. Decreased brain energy metabolic capacity has been recently related to a more efficient oxidative metabolism associated with underlying processes of synaptic plasticity, suggesting that a reduction in CCO activity is required for the stabilization of a preceding consolidated spatial cognitive mapping (Zorzo et al., 2021b). This might explain the better performance in

the experimental group. However, the particular molecular mechanisms associated with the effects of Y_2R blockade on regional brain oxidative metabolism are complex, involving the modulation of neuronal energy demands by the direct and indirect actions of NPY on different signalling systems, an issue that is difficult to disentangle. One possible mechanism is the action of NPY on other neurotransmitter systems (like catecholamines) and its regulation of glucose metabolism in both neurons and glial cells (Huang et al., 2021).

NPY Y_2R has been implicated with several neuronal excitability (Silva et al., 2005) and cognitive processes (Botterill et al., 2015; Hörmer et al., 2018; Verma et al., 2019); this suggests a functional role on spatial orientation. Specifically, when the NPY is applied before the memory training, it seems to impair the acquisition and retention of spatial memory, apparently via presynaptic Y_2R-mediated inhibition of synaptic glutamatergic transmission and LTP induction, [see review by Gøtzsche and Woldbye (2016)]. Y_2R receptors are present among others, in the DG granular cells (Schwarzer et al., 1998), and strong evidence shows that this receptor undergoes experience-dependent metaplastic regulation (Méndez-Couz et al., 2021), shifting from high affinity to low-affinity states of this receptor (Parker et al., 2007). The consequence of the inhibition of Y_2R receptors at glutamate terminals in the hippocampus would therefore be the rise in the glutamate release, but it remains unclear how this could support the improved hippocampus-dependent spatial learning. Under physiological conditions, the suppression of glutamate release by NPY acting on Y_2R receptors goes against information encoding through long-term potentiation. In turn, this blockade would favour the long-term depression (LTD), an intrinsic component of the acquisition of complex representations (Kemp & Manahan-Vaughan, 2004, 2007, 2008), which has been related to improvement in the water maze performance (Dong et al., 2013). The Y_2R-mediated LTD would be associated with higher synaptic plasticity and the observed retrieval improvement in the water maze task after the Y_2R blockade. In agreement, spatial

457 memory in the Barnes test was enhanced after Y_2R suppression; moreover, after hippocampal
458 reactivation in a Y_2R knockout rat model, the improved spatial memory was reduced (Hörmer
459 et al., 2018).

460 Remembering a past event involves the reactivation and partial modification of the patterns
461 of neural activity present at encoding (Richards & Frankland, 2017). In this regard, we had
462 previously reported a modified mPFC-dorsal hippocampus functional coupling involvement
463 during the acquisition and retrieval of a spatial memory task (Conejo et al., 2010; Conejo et
464 al., 2013; Méndez-Couz et al., 2015a).

465 We found that blockade of Y_2R receptors prior to a spatial memory retrieval test increases the
466 dDG metabolic activity. The dDG receives projections from the medial entorhinal cortex
467 (Wyss, 1981) and forms part of the circuits encoding for the “what” and “where” aspects of
468 context-dependent learning (Hoang et al., 2018). Recently, it has been proposed that the DG
469 is functionally involved in the discrimination between temporal and spatial experiences, due
470 to the strong segregation of information encoding in its upper and lower blades (Hoang et al.,
471 2018; Strauch & Manahan-Vaughan, 2020). In a contextual-dependent spatial task performed
472 in the T-maze (Méndez-Couz et al., 2019), increased IEG expression in the dDG lower blade
473 was reported, consistent with its recruitment by the recall of context-dependent or “where”
474 information encoding. Converging evidence suggests that dentate gyrus cell interconnectivity
475 is also essential for memory recall and its precision over time (Haubrich & Nader, 2018).
476 Taken together, the observed metabolic state change in the DG of experimental rats is
477 consistent with the DG critical involvement needed for an effective and precise recall of an
478 already known place (Emerich & Walsh, 1989; Méndez-Couz et al., 2015a; Zorzo et al.,
479 2021a).

A significant decrease of the ventral CA1 metabolic activity was found after dorsal hippocampal Y_2R antagonism. Whereas the dorsal portion of the hippocampus is mainly related to cognitive processing, the ventral pole has been traditionally associated with emotional and bodily states (Fanselow & Dong, 2010). Therefore, one could be tempted to interpret the differences in CCO activation found in this area as those typically related to the drug-infusion effect on anxiety or stress responses. However, consistently with the lack of anxiogenic or anxiolytic effects in this model (Méndez-Couz et al., 2021), no differences in mean CCO activity were found in brain regions typically associated with stress and anxiety, like the amygdala (Villarreal et al., 2002). Although the role of the ventral CA1 in spatial memory is not entirely clear, these metabolic results would agree with previous metabolic, electrophysiological and IEG studies pointing towards the involvement of the ventral hippocampus in rewarded spatial memory (Beer et al., 2014; Méndez-Couz et al., 2016; Sosa et al., 2020).

Besides, our results showed a metabolic activity decrease in the mammillary bodies after hippocampal Y_2R blockade. This diencephalic structure is crucial for transmitting information to higher forebrain centres via the mammillothalamocortical pathway, being involved in the neural circuitry for the recollection of memories (Guillery, 1955; Vann, 2005, 2010). Consistently, lower activity in the MM was also found after spatial memory extinction of a task previously acquired in the MWM (Méndez-Couz et al., 2014; Méndez-Couz et al., 2016), which is not surprising, taking into account that the mammillary bodies have been conventionally considered a hippocampal relay. Indeed, spatial memory deficits were observed after lesions in the mammillary bodies or their major efferent, the mammillothalamic tract (Vann, 2010).

Lastly, a lower CCO activity was observed in the infralimbic region of the mPFC. We have previously found decreased levels of Y_2R and increased Y_1R expression in the mPFC,

505 following hippocampal Y_2R antagonism and after the MWM task (Méndez-Couz et al.,
506 2021). These results were not surprising, given that the continued and intrinsic increase in
507 hippocampal excitability changes the excitation-inhibition equilibrium in the mPFC by
508 modifying GABA receptor expression (Grüter et al., 2015). Additionally, the Y_2R
509 antagonism causes disinhibition of glutamatergic and noradrenergic terminals in the
510 hippocampus that might change the excitatory output from the hippocampus to the mPFC.
511 This, in turn, may have triggered the changes in the metabolic activity of the IL cortex that
512 we detected in the experimental group.

513 At a metabolic level, changes in the mPFC have been found at the late stages of acquisition
514 (Conejo et al., 2010), retrieval (Zorzo et al., 2021a; 2021b) and the extinction of spatial
515 memory tasks in the water maze (Méndez-Couz et al., 2014, 2015b). During early recall, the
516 metabolic activation in the dDG of the hippocampus is negatively correlated with the
517 metabolic levels measured in the IL cortex (Méndez-Couz et al., 2015a), which would fit
518 with our results in the experimental group, showing a better performance associated with a
519 higher DG and a lower IL metabolic energy levels. However, given the mediation of the
520 mPFC in the attentional and motivational components of the spatial orientation in the MWM
521 (Conejo et al., 2007; Conejo et al., 2010), one cannot rule out the possibility of motivational
522 aspects influencing a better retrieval. In line with this interpretation, the IL cortex is reported
523 to modulate appetitive Pavlovian extinction (Mendoza et al., 2015) and extinction learning of
524 a spatial memory task (Méndez-Couz et al., 2014), in which the persistence of the previously
525 reinforced learned response needed to be decreased. This aspect of mPFC function, together
526 with the above-mentioned rapid NPY metaplastic changes in the hippocampal-mPFC circuit,
527 may account for the improved spatial memory recall observed in experimental rats after the
528 Y_2R antagonist administration.

Our results help to further illuminate the role of the NPY system in spatial learning. We demonstrate that under hippocampal Y_2R antagonism, spatial memory recall is enhanced and that such enhancement is correlated with changes in regional brain energy metabolism along the dorso-ventral axis of the hippocampus, the medial mammillary bodies and the infralimbic region of the mPFC. Taken together, these results suggest that Y_2R exert control over patterns of brain activation that are relevant for spatial memory expression.

Author Contributions

The study was designed by NC and MM-C. Experiments were conducted by MM-C, HGP and NC, and analysed by all authors. MM-C and NC interpreted the results and wrote the article.

Acknowledgements

We gratefully thank Prof. Ana Paula Silva for providing the Y_2R receptor antagonist.

Funding Sources

This work was supported by the following grants: MINECO, Spain [grant numbers PSI2017-83038-P, PSI 2017-83893-R and PSI2017□90806□REDT].

Statement of Ethics

All experimental procedures carried out with animals were approved by the local Animal Ethics Committee of the University of Oviedo and following the European Communities Council Directive 2010/63/UE and the Spanish legislation on care and use of animals for experimentation (Royal Decree 53/2013). All efforts were made to minimize the number of animals used and their suffering.

1. FIGURE LEGENDS

Figure 1: **Experiment timeline and behavioural procedure**. **Top)** Temporal line of the procedure. **Middle)** After recovery from surgery, rats were trained in a reference spatial memory task in the water maze for two days. On the first day, they went through four sessions of four trials. Meanwhile, on the second day, three sessions of four trials each were carried out. After the last trial of the acquisition, a transfer test, to determine the virtual quadrant preference of the rats, was performed. An additional trial was carried out in which the platform was placed in its original position, to avoid early extinction of the acquired task. One day after the acquisition was complete, rats received intrahippocampal infusion with the Y_2R selective antagonist (1 nmoL/µL BIIE0246 in 0.9% physiological saline +1% DMSO) or vehicle saline solution, 30 min before the retrieval test in the water maze. Treated rats underwent four trials with the platform in the maze and an additional transfer test without the platform. **Bottom)** Position of the platform in the different stages of the water maze task. In the pretraining phase, the platform was visible, 2 cm above the water surface. During acquisition, the platform was hidden in the maze; rats orientated themselves through distal cues situated in panels situated around the maze. For the retention probe after the acquisition, the platform was removed from the maze. The time to reach the platform (escape latencies) and the time that rats spent in the virtual reinforced quadrant area during the transfer memory probe test were taken as variables related to spatial learning and memory performance.

Figure 2: After treatment, rats required less time to reach the platform. a) Acquisition learning curve. Rats learned the hidden platform spatial task. Differences along the training sessions 1 to 7 were found, showing a typical learning curve with decreasing mean latencies needed to reach the platform ($p<0.001$). The acquisition was stopped at Session 7 after achieving, on average, the learning criterion of 20 s to reach the platform, represented by a dashed line. **b) Latencies post-treatment.** One day after the task was successfully acquired,

576 the spatial memory test took place, Y_2R antagonist (for the experimental group) or vehicle
577 saline solution (for the saline control group) was infused 30 min prior to a spatial memory
578 test was performed. Experimental and vehicle groups presented significant differences in the
579 latency needed to reach the platform $^{+}$(p=0.001); specifically, the treated group needed less
580 time to reach the platform as compared to the vehicle saline control in the first trial, although
581 both groups reached low latencies at the end of the retrieval test. The average amount of time
582 spent is represented in bars, dots represent individual data points.

583 **Figure 3: Treated rats spent more time in the reinforced quadrant after treatment than**
584 **vehicle saline controls.** Mean time spent in the virtual quadrants in which the maze was
585 divided **a)** At the end of the acquisition phase, rats spent more time in the previously
586 reinforced quadrant as compared to the rest of the quadrants. **b)** After the saline/drug infusion
587 on the test day, the vehicle saline group spent more time in the reinforced quadrant as
588 compared to A and D; meanwhile, the experimental group spent more time in the reinforced
589 quadrant than in all the rest. When groups were compared, the NPY Y_2R antagonist treated
590 rats spent more time in the reinforced quadrant as compared to the vehicle control *(p<0.05)
591 ++(p<0.001) +(p<0.01)

592 **Figure 4: Brain metabolism was increased in the dorsal dentate gyrus and decreased in**
593 **the ventral CA1, the mammillary bodies and the IL region of the mPFC after Y_2R**
594 **blockade prior to spatial memory retrieval**. **a,b)** cytochrome c oxidase (CCO) activity
595 results. Bars represent the mean ± S.E.M for each group. ** (p<0.05) experimental *vs* control
596 and saline groups; $^{+}$ (p<0.01) control cage *vs* experimental group. **c-f)** Representative images
597 of CCO histochemical stain performed in vehicle control and experimental groups showing:
598 **c)** the prefrontal cortex (bregma 4.20 to 3.72 mm), **d)** dorsal hippocampus (bregma -2.64 mm
599 to -3.72 mm), **e)** the mammillary bodies (bregma -4.2 mm to -4.68 mm) and **f)** the ventral
600 hippocampus (bregma -4.8 mm to -5.28 mm) according to Paxinos and Watson (2004); for

601 the exact values found in experimental, vehicle and control cage, please refer to Table 1.
602 Black or red colours represent higher CCO activity, while green to blue colours symbolize
603 lower activity. Scale bar: 1mm. The relative optical density of each region was measured by
604 taking three non-overlapping readings in each section, in three consecutive sections by using
605 a square-shaped sampling window adjusted for each region size (MCID, InterFocus Imaging
606 Ltd., Linton, England). 150 x 150 mm (96 x 96 DPI). Abbreviations: CC (control cage
607 group), Exp (Experimental group), Veh (Vehicle group), dorsal dentate gyrus (dDG), ventral
608 (vDG), dorsal and ventral *Cornu Ammonis* 3 (dCA3, vCA3 respectively), dorsal and ventral
609 *Cornu Ammonis* 1 (dCA1, vCA1 respectively), medial nucleus of the mammillary bodies
610 (MM) and lateral nucleus (LM).
611
612
613
614
615
616
617
618
619
620
621
622
623
624
625

REFERENCES

Agin, V., Chicher, R., & Chichery, M. P. (2001). Effects of learning on cytochrome oxidase activity in cuttlefish brain. *NeuroReport*, *12*(1), 113–116. https://doi.org/10.1097/00001756-200101220-00030, PubMed: 11201069.

Almeida, A., Moncada, S., & Bolaños, J. P. (2004). Nitric oxide switches on glycolysis through the AMP protein kinase and 6-phosphofructo-2-kinase pathway. *Nature Cell Biology*, *6*(1), 45–51- https://doi.org/10.1038/ncb1080

Balasubramanian, N., Sagarkar, S., Jadhav, M., Shahi, N., Sirmaur, R., & Sakharkar, A. J. (2021). Role for histone deacetylation in traumatic brain injury-induced deficits in neuropeptide Y in arcuate nucleus: Possible implications in feeding behavior. *Neuroendocrinology*, 111(12), 1187–1200. https://doi.org/10.1159/000513638

Beer, Z., Chwiesko, C., & Sauvage, M. M. (2014). Processing of spatial and non-spatial information reveals functional homogeneity along the dorso-ventral axis of CA3, but not CA1. *Neurobiology of Learning and Memory*, *111*, 56–64. https://doi.org/10.1016/j.nlm.2014.03.001

Bertocchi, I., Mele, P., Ferrero, G., Oberto, A., Carulli, D., & Eva, C. (2021). NPY-Y1 receptor signaling controls spatial learning and perineuronal net expression. *Neuropharmacology*, *184*, 108425. https://doi.org/10.1016/j.neuropharm.2020.108425.

Bertoni-Freddari, C., Fattoretti, P., Casoli, T., Di Stefano, G., Solazzi, M., Gracciotti, N., & Pompei, P. (2001). Mapping of mitochondrial metabolic competence by cytochrome oxidase and succinic dehydrogenase cytochemistry. *Journal of Histochemistry and Cytochemistry*, *49*(9), 1191–1192. https://doi.org/10.1177/002215540104900915

649 Billington, C. J., & Levine, A. S. (1992). Hypothalamic neuropeptide Y regulation of feeding
650 and energy metabolism. *Current Opinion in Neurobiology, 2*(6), 847–851.
651 https://doi.org/10.1016/0959-4388(92)90144-a
652 Botterill, J. J., Guskjolen, A. J., Marks, W. N., Caruncho, H. J., & Kalynchuk, L. E. (2015).
653 Limbic but not non-limbic kindling impairs conditioned fear and promotes plasticity
654 of NPY and its Y2 receptor. *Brain Structure and Function, 220*(6), 3641–3655.
655 https://doi.org/10.1007/s00429-014-0880-z
656 Brown, G. C. (2007). Mechanisms of inflammatory neurodegeneration: iNOS and NADPH
657 oxidase. *Biochemical Society Transactions, 35*(5), 1119–1121.
658 https://doi.org/10.1042/BST0351119
659 Bures, J., Buresova, A., & Huston, J. (1976). Innate and motivated behaviour. In J. Bures
660 (Ed.), *Techniques and basic experiments for a study of Brain and behavior* (pp. 37–
661 45). Elsevier.
662 Chicherin, I. V., Dashinimaev, E., Baleva, M., Krasheninnikov, I., Levitskii, S., & Kamenski,
663 P. (2019). Cytochrome c oxidase on the crossroads of transcriptional regulation and
664 bioenergetics. *Frontiers in Physiology, 10*, 644.
665 https://doi.org/10.3389/fphys.2019.00644
666 Comeras, L. B., Herzog, H., & Tasan, R. O. (2019). Neuropeptides at the crossroad of fear
667 and hunger: A special focus on neuropeptide Y. *Annals of the New York Academy of*
668 *Sciences, 1455*(1), 59–80. https://doi.org/10.1111/nyas.14179
669 Conejo, N. M., Cimadevilla, J. M., González-Pardo, H., Méndez-Couz, M., & Arias, J. L.
670 (2013). Hippocampal inactivation with TTX impairs long-term spatial memory
671 retrieval and modifies brain metabolic activity. *PLOS ONE, 8*(5), e64749.
672 https://doi.org/10.1371/journal.pone.0064749

673 Conejo, N. M., González-Pardo, H., Gonzalez-Lima, F., & Arias, J. L. (2010). Spatial
674 learning of the water maze: Progression of brain circuits mapped with cytochrome
675 oxidase histochemistry. *Neurobiology of Learning and Memory*, *93*(3), 362–371.
676 https://doi.org/10.1016/j.nlm.2009.12.002
677 Conejo, N. M., González-Pardo, H., Vallejo, G., & Arias, J. L. (2007). Changes in brain
678 oxidative metabolism induced by water maze training. *Neuroscience*, *145*(2), 403–
679 412. https://doi.org/10.1016/j.neuroscience.2006.11.057
680 Decressac, M., & Barker, R. A. (2012). Neuropeptide Y and its role in CNS disease and
681 repair. *Experimental Neurology*, *238*(2), 265–272.
682 https://doi.org/10.1016/j.expneurol.2012.09.004
683 Dong, Z., Bai, Y., Wu, X., Li, H., Gong, B., Howland, J. G., Huang, Y., He, W., Li, T., &
684 Wang, Y. T. (2013). Hippocampal long-term depression mediates spatial reversal
685 learning in the Morris water maze. *Neuropharmacology*, *64*, 65–73.
686 https://doi.org/10.1016/j.neuropharm.2012.06.027
687 dos Santos, V. V., Santos, D. B., Lach, G., Rodrigues, A. L., Farina, M., De Lima, T. C., &
688 Prediger, R. D. (2013). Neuropeptide Y (NPY) prevents depressive-like behavior,
689 spatial memory deficits and oxidative stress following amyloid-beta (Aβ (1–40))
690 administration in mice. *Behavioural Brain Research*, *244*, 107–115.
691 https://doi.org/10.1016/j.bbr.2013.01.039
692 Emerich, D. F., & Walsh, T. J. (1989). Selective working memory impairments following
693 intradentate injection of colchicine: Attenuation of the behavioral but not the
694 neuropathological effects by gangliosides GM1 and AGF2. *Physiology and Behavior*,
695 *45*(1), 93–101. https://doi.org/10.1016/0031-9384(89)90170-4

696 Fanselow, M. S., & Dong, H. W. (2010). Are the dorsal and ventral hippocampus
697 functionally distinct structures? *Neuron*, *65*(1), 7–19.
698 https://doi.org/10.1016/j.neuron.2009.11.031, PubMed: 20152109.
699 Ferreira, R., Xapelli, S., Santos, T., Silva, A. P., Cristóvão, A., Cortes, L., & Malva, J. O.
700 (2010). Neuropeptide Y Modulation of interleukin-1beta (IL-1beta)-induced nitric
701 oxide Production in Microglia. *Journal of Biological Chemistry*, *285*(53), 41921–
702 41934. https://doi.org/10.1074/jbc.M110.164020
703 Flood, J. F., Hernandez, E. N., & Morley, J. E. (1987). Modulation of memory processing by
704 neuropeptide Y. *Brain Research*, *421*(1–2), 280–290. https://doi.org/10.1016/0006-
705 8993(87)91297-2
706 Furtinger, S., Pirker, S., Czech, T., Baumgartner, C., Ransmayr, G., & Sperk, G. (2001).
707 Plasticity of Y1 and Y2 receptors and neuropeptide Y fibers in patients with temporal
708 lobe epilepsy. *Journal of Neuroscience*, *21*(15), 5804–5812.
709 https://doi.org/10.1523/JNEUROSCI.21-15-05804.2001
710 Gasalla, P., Begega, A., Soto, A., Dwyer, D. M., & López, M. (2016). Functional brain
711 networks underlying latent inhibition of conditioned disgust in rats. *Behavioural*
712 *Brain Research*, *315*, 36–44. https://doi.org/10.1016/j.bbr.2016.07.051
713 Gobbi, M., Gariboldi, M., Piwko, C., Hoyer, D., Sperk, G., & Vezzani, A. (1998). Distinct
714 changes in peptide YY binding to, and mRNA levels of, Y1 and Y2 receptors in the
715 rat hippocampus associated with kindling epileptogenesis. *Journal of Neurochemistry*,
716 *70*(4), 1615–1622. https://doi.org/10.1046/j.1471-4159.1998.70041615.x
717 Gonçalves, J., Martins, J., Baptista, S., Ambrósio, A. F., & Silva, A. P. (2016). Effects of
718 drugs of abuse on the central neuropeptide Y system. *Addiction Biology*, 21(4), 755–
719 765. https://doi.org/10.1111/adb.12250

720 Gonçalves, J., Ribeiro, C. F., Malva, J. O., & Silva, A. P. (2012). Protective role of
721 neuropeptide Y Y_2 receptors in cell death and microglial response following
722 methamphetamine injury. *European Journal of Neuroscience*, *36*(9), 3173–3183.
723 https://doi.org/10.1111/j.1460-9568.2012.08232.x
724 Gonzalez-Lima, F., & Cada, A. (1994). Cytochrome oxidase activity in the auditory system
725 of the mouse: A qualitative and quantitative histochemical study. *Neuroscience*,
726 *63*(2), 559–578. https://doi.org/10.1016/0306-4522(94)90550-9
727 Gonzalez-Lima, F., & Jones, D. (1994). Quantitative mapping of cytochrome oxidase activity
728 in the central auditory system of the gerbil: A study with calibrated activity standards
729 and metal-intensified histochemistry. *Brain Research*, *660*(1), 34–49.
730 https://doi.org/10.1016/0006-8993(94)90836-2
731 Gøtzsche, C. R., & Woldbye, D. P. (2016). The role of NPY in learning and memory.
732 *Neuropeptides*, *55*, 79–89. https://doi.org/10.1016/j.npep.2015.09.010.
733 Grüter, T., Wiescholleck, V., Dubovyk, V., Aliane, V., & Manahan-Vaughan, D. (2015).
734 Altered neuronal excitability underlies impaired hippocampal function in an animal
735 model of psychosis. *Frontiers in Behavioral Neuroscience*, *9*, 117.
736 https://doi.org/10.3389/fnbeh.2015.00117
737 Guillery, R. W. (1955). A quantitative study of the mamillary bodies and their connexions.
738 *Journal of Anatomy*, *89*(1), 19–32. PubMed: 14353794.
739 Haigh, J. L., New, L. E., & Filippi, B. M. (2020). Mitochondrial dynamics in the brain are
740 associated with feeding, glucose homeostasis, and whole-body metabolism. *Frontiers*
741 *in Endocrinology (Lausanne)*, *11*, 580879. https://doi.org/10.3389/fendo.2020.580879
742 Haubrich, J., & Nader, K. (2018). A molecular mechanism governing memory precision.
743 *Nature Medicine*, *24*(4), 390–391. https://doi.org/10.1038/nm.4532

744 Hescham, S., Temel, Y., Casaca-Carreira, J., Arslantas, K., Yakkioui, Y., Blokland, A., &
745 Jahanshahi, A. (2014). A neuroanatomical analysis of the effects of a memory
746 impairing dose of scopolamine in the rat brain using cytochrome c oxidase as
747 principle marker. *Journal of Chemical Neuroanatomy*, *59–60*, 1–7.
748 https://doi.org/10.1016/j.jchemneu.2014.04.001
749 Hoang, T. H., Aliane, V., & Manahan-Vaughan, D. (2018). Novel encoding and updating of
750 positional, or directional, spatial cues are processed by distinct hippocampal subfields:
751 Evidence for parallel information processing and the "what" stream. *Hippocampus*,
752 *28*(5), 315–326. https://doi.org/10.1002/hipo.22833
753 Hörmer, B. A., Verma, D., Gasser, E., Wieselthaler-Hölzl, A., Herzog, H., & Tasan, R. O.
754 (2018). Hippocampal NPY Y2 receptors modulate memory depending on emotional
755 valence and time. *Neuropharmacology*, *143*, 20–28.
756 https://doi.org/10.1016/j.neuropharm.2018.09.018
757 Huang, Y., Lin, X., & Lin, S. (2021). Neuropeptide Y and metabolism syndrome: An update
758 on perspectives of clinical therapeutic intervention strategies. *Frontiers in Cell and*
759 *Developmental Biology*, *9*, 695623. https://doi.org/10.3389/fcell.2021.695623
760 Kemp, A., & Manahan-Vaughan, D. (2004). Hippocampal long-term depression and long-
761 term potentiation encode different aspects of novelty acquisition. *Proceedings of the*
762 *National Academy of Sciences of the United States of America*, *101*(21), 8192–8197.
763 https://doi.org/10.1073/pnas.0402650101
764 Kemp, A., & Manahan-Vaughan, D. (2007). Hippocampal long-term depression: Master or
765 minion in declarative memory processes? *Trends in Neurosciences*, *30*(3), 111–118.
766 https://doi.org/10.1016/j.tins.2007.01.002

767 Kemp, A., & Manahan-Vaughan, D. (2008). The hippocampal CA1 region and dentate gyrus
768 differentiate between environmental and spatial feature encoding through long-term
769 depression. *Cerebral Cortex*, *18*(4), 968–977. https://doi.org/10.1093/cercor/bhm136
770 Kornhuber, J., & Zoicas, I. (2017). Neuropeptide Y prolongs non-social memory and
771 differentially affects acquisition, consolidation, and retrieval of non-social and social
772 memory in male mice [Sci. rep., *6821*, 6821]. *Scientific Reports*, 7(1), 6821.
773 https://doi.org/10.1038/s41598-017-07273-x
774 Kornhuber, J., & Zoicas, I. (2020). Neuropeptide Y prolongs non-social memory in a brain
775 region- and receptor-specific way in male mice. *Neuropharmacology*, *175*, 108199.
776 https://doi.org/10.1016/j.neuropharm.2020.108199
777 Malva, J. O., Xapelli, S., Baptista, S., Valero, J., Agasse, F., Ferreira, R., & Silva, A. P.
778 (2012). Multifaces of neuropeptide Y in the brain—Neuroprotection, neurogenesis
779 and neuroinflammation. *Neuropeptides*, *46*(6), 299–308.
780 https://doi.org/10.1016/j.npep.2012.09.001
781 Méndez-Couz, M., Becker, J. M., & Manahan-Vaughan, D. (2019). Functional
782 compartmentalization of the contribution of hippocampal subfields to context-
783 dependent extinction learning. *Frontiers in Behavioral Neuroscience*, *13*, 256.
784 https://doi.org/10.3389/fnbeh.2019.00256
785 Méndez-Couz, M., Conejo, N. M., González-Pardo, H., & Arias, J. L. (2015a). Functional
786 interactions between dentate gyrus, striatum and anterior thalamic nuclei on spatial
787 memory retrieval. *Brain Research*, *1605*, 59–69.
788 https://doi.org/10.1016/j.brainres.2015.02.005
789 Méndez-Couz, M., Conejo, N. M., Vallejo, G., & Arias, J. L. (2014). Spatial memory
790 extinction: A c-Fos protein mapping study. *Behavioural Brain Research*, *260*, 101–
791 110. https://doi.org/10.1016/j.bbr.2013.11.032

792 Méndez-Couz, M., Conejo, N. M., Vallejo, G., & Arias, J. L. (2015b). Brain functional
793 network changes following prelimbic area inactivation in a spatial memory extinction
794 task. *Behavioural Brain Research*, 287, 247–255.
795 https://doi.org/10.1016/j.bbr.2015.03.033
796 Méndez-Couz, M., González-Pardo, H., Vallejo, G., Arias, J. L., & Conejo, N. M. (2016).
797 Spatial memory extinction differentially affects dorsal and ventral hippocampal
798 metabolic activity and associated functional brain networks. *Hippocampus*, *26*(10),
799 1265–1275. https://doi.org/10.1002/hipo.22602
800 Méndez-Couz, M., Manahan-Vaughan, D., Silva, A. P., González-Pardo, H., Arias, J. L., &
801 Conejo, N. M. (2021). Metaplastic contribution of neuropeptide Y receptors to spatial
802 memory acquisition. *Behavioural Brain Research*, *396*, 112864.
803 https://doi.org/10.1016/j.bbr.2020.112864
804 Mendoza, J., Sanio, C., & Chaudhri, N. (2015). Inactivating the infralimbic but not prelimbic
805 medial prefrontal cortex facilitates the extinction of appetitive Pavlovian conditioning
806 in Long-Evans rats. *Neurobiology of Learning and Memory*, *118*, 198–208.
807 https://doi.org/10.1016/j.nlm.2014.12.006
808 Moncada, S., & Bolaños, J. P. (2006). Nitric oxide, cell bioenergetics and neurodegeneration.
809 *Journal of Neurochemistry*, *97*(6), 1676–1689. https://doi.org/10.1111/j.1471-
810 4159.2006.03988.x
811 Morán, J., Garrido, P., Alonso, A., Cabello, E., & González, C. (2013). 17 Beta-estradiol and
812 genistein acute treatments improve some cerebral cortex homeostasis aspects
813 deteriorated by aging in female rats. *Experimental Gerontology*, *48*(4), 414–421.
814 https://doi.org/10.1016/j.exger.2013.02.010

Morris, R. (1984). Developments of a water-maze procedure for studying spatial learning in the rat. *Journal of Neuroscience Methods*, *11*(1), 47–60. https://doi.org/10.1016/0165-0270(84)90007-4

Nwokafor, C., Serova, L. I., Nahvi, R. J., McCloskey, J., & Sabban, E. L. (2020). Activation of NPY receptor subtype 1 by [D-His26]NPY is sufficient to prevent development of anxiety and depressive like effects in the single prolonged stress rodent model of PTSD. *Neuropeptides*, *80*, 102001. https://doi.org/10.1016/j.npep.2019.102001

Parker, R. M., & Herzog, H. (1998). Comparison of Y-receptor subtype expression in the rat hippocampus. *Regulatory Peptides*, 75–76, 109–115. https://doi.org/10.1016/s0167-0115(98)00059-7

Parker, R. M., & Herzog, H. (1999). Regional distribution of Y-receptor subtype mRNAs in rat brain. *European Journal of Neuroscience*, *11*(4), 1431–1448. https://doi.org/10.1046/j.1460-9568.1999.00553.x

Parker, S. L., Parker, M. S., Sah, R., Balasubramaniam, A., & Sallee, F. R. (2007). Self-regulation of agonist activity at the Y receptors. *Peptides*, *28*(2), 203–213. https://doi.org/10.1016/j.peptides.2006.07.032

Paxinos, G., & Watson, C. (2004). *The Rat Brain in stereotaxic Coordinates-The New Coronal Set* (5th ed). Elsevier Academic Press.

Redrobe, J. P., Dumont, Y., Herzog, H., & Quirion, R. (2004). Characterization of neuropeptide Y, Y(2) receptor knockout mice in two animal models of learning and memory processing. *Journal of Molecular Neuroscience*, *22*(3), 159–166. https://doi.org/10.1385/JMN:22:3:159

Reichmann, F., & Holzer, P. (2016). Neuropeptide Y: A stressful review. *Neuropeptides*, *55*, 99–109. https://doi.org/10.1016/j.npep.2015.09.008

839 Richards, B. A., & Frankland, P. W. (2017). The persistence and transience of memory.
840 *Neuron*, *94*(6), 1071–1084. https://doi.org/10.1016/j.neuron.2017.04.037
841 Schwarzer, C., Kofler, N., & Sperk, G. (1998). Up-regulation of neuropeptide Y-Y2 receptors
842 in an animal model of temporal lobe epilepsy. *Molecular Pharmacology*, *53*(1), 6–13.
843 https://doi.org/10.1124/mol.53.1.6
844 Silva, A. P., Xapelli, S., Grouzmann, E., & Cavadas, C. (2005). The putative neuroprotective
845 role of neuropeptide Y in the central nervous system. *Current Drug Targets. CNS and*
846 *Neurological Disorders*, *4*(4), 331–347. https://doi.org/10.2174/1568007054546153.
847 Sosa, M., Joo, H. R., & Frank, L. M. (2020). Dorsal and ventral hippocampal sharp-wave
848 ripples activate distinct nucleus accumbens networks. *Neuron*, *105*(4), 725–741.e8.
849 https://doi.org/10.1016/j.neuron.2019.11.022
850 Stanić, D., Brumovsky, P., Fetissov, S., Shuster, S., Herzog, H., & Hökfelt, T. (2006).
851 Characterization of neuropeptide Y2 receptor protein expression in the mouse brain. I.
852 Distribution in cell bodies and nerve terminals. *Journal of Comparative Neurology*,
853 *499*(3), 357–390. https://doi.org/10.1002/cne.21046.
854 Stanić, D., Mulder, J., Watanabe, M., & Hökfelt, T. (2011). Characterization of NPY Y2
855 receptor protein expression in the mouse brain. II. Coexistence with NPY, the Y1
856 receptor, and other neurotransmitter-related molecules. *Journal of Comparative*
857 *Neurology*, *519*(7), 1219–1257. https://doi.org/10.1002/cne.22608
858 Stanley, B. G., & Leibowitz, S. F. (1984). Neuropeptide Y: Stimulation of feeding and
859 drinking by injection into the paraventricular nucleus. *Life Sciences*, *35*(26), 2635–
860 2642. https://doi.org/10.1016/0024-3205(84)90032-8
861 Strauch, C., & Manahan-Vaughan, D. (2020). Orchestration of hippocampal information
862 encoding by the piriform cortex. *Cerebral Cortex*, *30*(1), 135–147.
863 https://doi.org/10.1093/cercor/bhz077

Su, Y., Foppen, E., Fliers, E., & Kalsbeek, A. (2016). Effects of intracerebroventricular administration of neuropeptide Y on metabolic gene expression and energy metabolism in male rats. *Endocrinology*, *157*(8), 3070–3085. https://doi.org/10.1210/en.2016-1083

Tasan, R. O., Verma, D., Wood, J., Lach, G., Hörmer, B., de Lima, T. C., Herzog, H., & Sperk, G. (2016). The role of neuropeptide Y in fear conditioning and extinction. *Neuropeptides*, *55*, 111–126. https://doi.org/10.1016/j.npep.2015.09.007

Tatemoto, K. (1982). Neuropeptide Y: Complete amino acid sequence of the brain peptide. *Proceedings of the National Academy of Sciences of the United States of America*, *79*(18), 5485–5489. https://doi.org/10.1073/pnas.79.18.5485

Thomas, J. R., & Ahlers, S. T. (1991). Neuropeptide-Y both improves and impairs delayed matching-to-sample performance in rats. *Pharmacology, Biochemistry, and Behavior*, *40*(2), 417–422. https://doi.org/10.1016/0091-3057(91)90573-k

Thorsell, A., Michalkiewicz, M., Dumont, Y., Quirion, R., Caberlotto, L., Rimondini, R., Mathe, A. A., & Heilig, M. (2000). Behavioral insensitivity to restraint stress, absent fear suppression of behavior and impaired spatial learning in transgenic rats with hippocampal neuropeptide Y overexpression. *Proceedings of the National Academy of Sciences of the United States of America*, *97*(23), 12852–12857. https://doi.org/10.1073/pnas.220232997

Tschenett, A., Singewald, N., Carli, M., Balducci, C., Salchner, P., Vezzani, A., Herzog, H., & Sperk, G. (2003). Reduced anxiety and improved stress coping ability in mice lacking NPY-Y2 receptors. *European Journal of Neuroscience*, *18*(1), 143–148. https://doi.org/10.1046/j.1460-9568.2003.02725.x

887 Vann, S. D. (2005). Transient spatial deficit associated with bilateral lesions of the lateral
888 mammillary nuclei. *European Journal of Neuroscience*, *21*(3), 820–824.
889 https://doi.org/10.1111/j.1460-9568.2005.03896.x
890 Vann, S. D. (2010). Re-evaluating the role of the mammillary bodies in memory.
891 *Neuropsychologia*, *48*(8), 2316–2327.
892 https://doi.org/10.1016/j.neuropsychologia.2009.10.019
893 Vázquez-León, P., Ramírez-San Juan, E., Marichal-Cancino, B. A., Campos-Rodríguez, C.,
894 Chávez-Reyes, J., & Miranda-Páez, A. (2020). NPY-Y1 receptors in dorsal
895 periaqueductal gray modulate anxiety, alcohol intake, and relapse in Wistar rats.
896 *Pharmacology, Biochemistry, and Behavior*, *199*, 173071.
897 https://doi.org/10.1016/j.pbb.2020.173071.
898 Verma, D., Jamil, S., Tasan, R. O., Lange, M. D., & Pape, H. C. (2019). Single stimulation of
899 Y2 receptors in BNSTav facilitates extinction and dampens reinstatement of fear.
900 *Psychopharmacology*, *236*(1), 281–291. https://doi.org/10.1007/s00213-018-5080-8
901 Villarreal, J. S., Gonzalez-Lima, F., Berndt, J., & Barea-Rodriguez, E. J. (2002). Water maze
902 training in aged rats: Effects on brain metabolic capacity and behavior. *Brain*
903 *Research*, *939*(1–2), 43–51. https://doi.org/10.1016/s0006-8993(02)02545-3
904 Wong-Riley, M. T. (1989). Cytochrome oxidase: An endogenous metabolic marker for
905 neuronal activity. *Trends in Neurosciences*, *12*(3), 94–101.
906 https://doi.org/10.1016/0166-2236(89)90165-3
907 Wong-Riley, M. T. (2012). Bigenomic regulation of cytochrome c oxidase in neurons and the
908 tight coupling between neuronal activity and energy metabolism. *Advances in*
909 *Experimental Medicine and Biology*, *748*, 283–304. https://doi.org/10.1007/978-1-
910 4614-3573-0_12

911 Wyss, J. M. (1981). An autoradiographic study of the efferent connections of the entorhinal
912 cortex in the rat. *Journal of Comparative Neurology*, *199*(4), 495–512.
913 https://doi.org/10.1002/cne.901990405
914 Xapelli, S., Agasse, F., Ferreira, R., Silva, A. P., & Malva, J. O. (2006). Neuropeptide Y as
915 an endogenous antiepileptic, neuroprotective and pro-neurogenic peptide. *Recent*
916 *Patents on CNS Drug Discovery*, *1*(3), 315–324.
917 https://doi.org/10.2174/157488906778773689
918 Zambello, E., Zanetti, L., Hédou, G. F., Angelici, O., Arban, R., Tasan, R. O., Sperk, G., &
919 Caberlotto, L. (2011). Neuropeptide Y-Y2 receptor knockout mice: Influence of
920 genetic background on anxiety-related behaviors. *Neuroscience*, *176*, 420–430.
921 https://doi.org/10.1016/j.neuroscience.2010.10.075
922 Zorzo, C., Arias, J. L., & Méndez, M. (2021a). Hippocampus and cortex are involved in the
923 retrieval of a spatial memory under full and partial cue availability. *Behavioural Brain*
924 *Research*, *405*, 113204. https://doi.org/10.1016/j.bbr.2021.113204.
925 Zorzo, C., Arias, J. L., & Méndez, M. (2021b). Recovering spatial information through
926 reactivation: Brain oxidative metabolism involvement in males and females.
927 *Neuroscience*, *459*, 1–15. https://doi.org/10.1016/j.neuroscience.2021.02.002
928
929
930

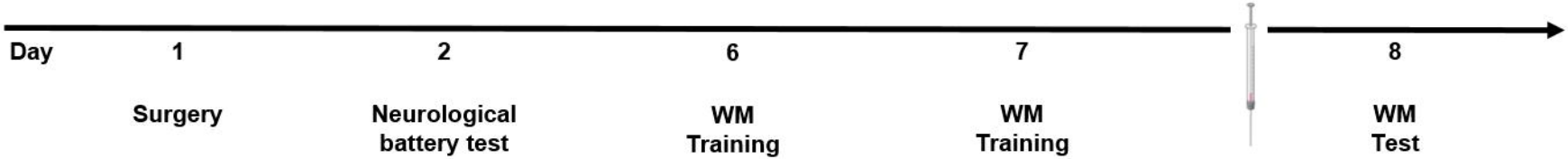
Day
1
2
6
7
8
Surgery
Neurological battery test
WM Training
WM Training
WM Test
• Pretraining
• 4 sessions /4 trials
• 3 sessions/4 trials
• Retention probe
• Post-retention trial
• 1 session /4 trials
• Retention probe
Platform position
A
C
D
B
Pretraining
Training
Test
Post-retention
Retention

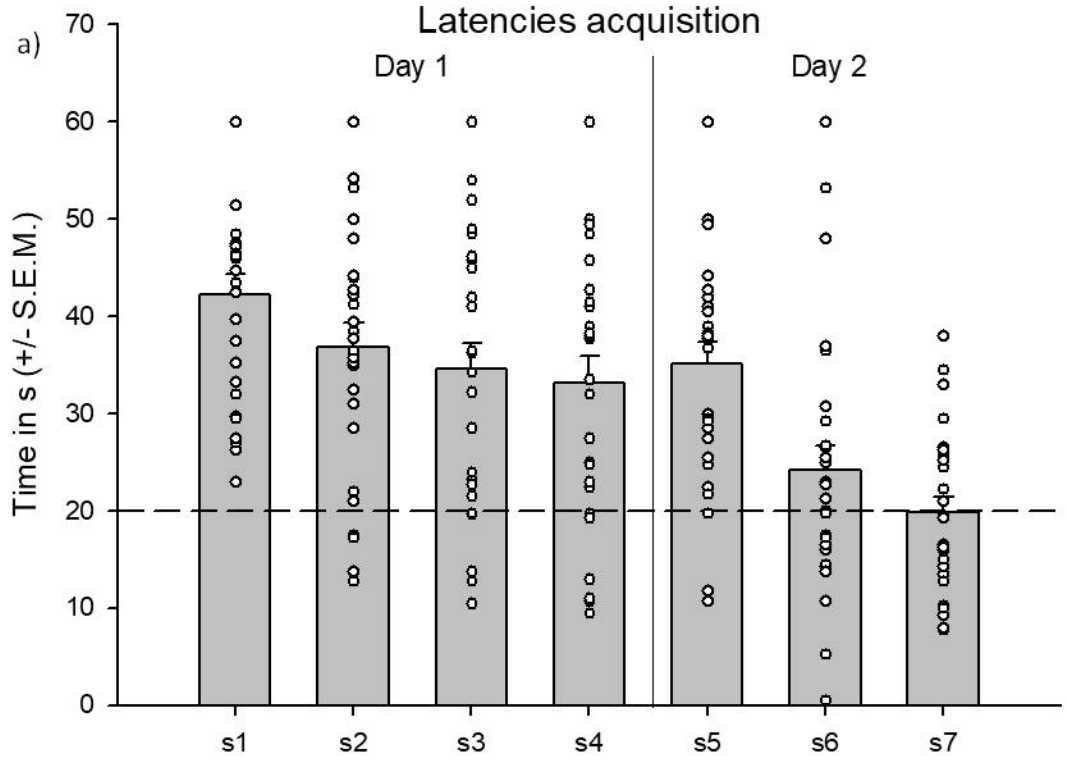
a)
Latencies acquisition
Day 1
Day 2
Time in s (+/- S.E.M.)
70
60
50
40
30
20
10
0
s1
s2
s3
s4
s5
s6
s7

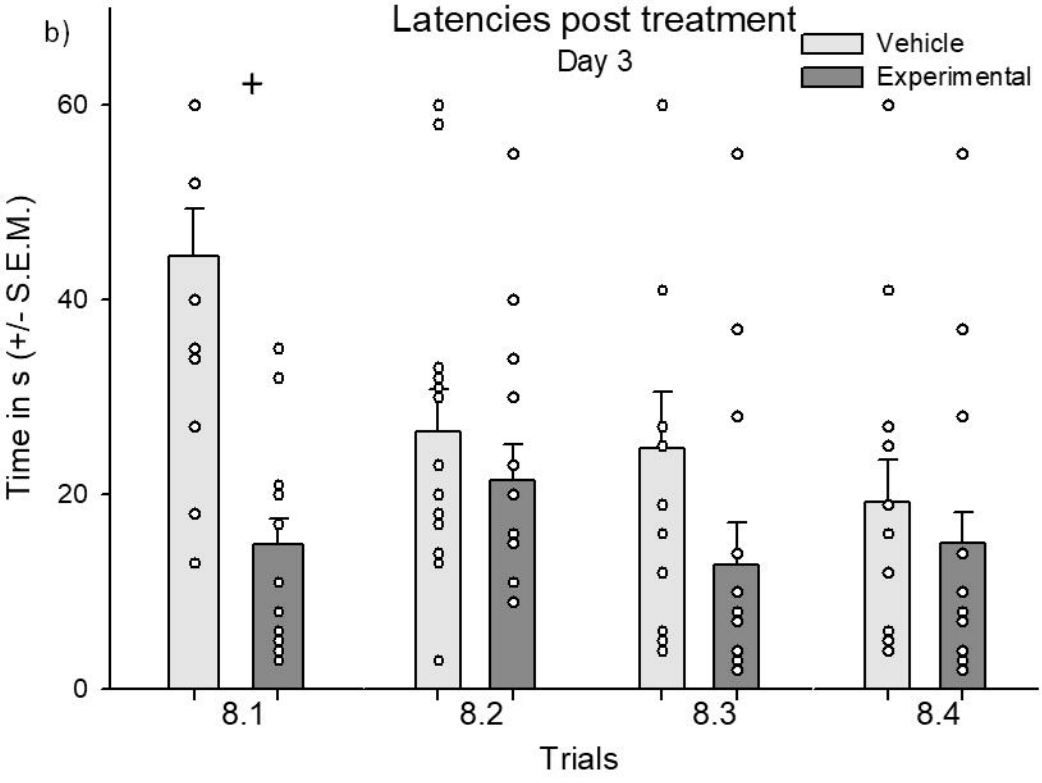
b)
Latencies post treatment
Day 3
Vehicle
Experimental
Time in s (+/- S.E.M.)
60
40
20
0
8.1
8.2
8.3
8.4
Trials

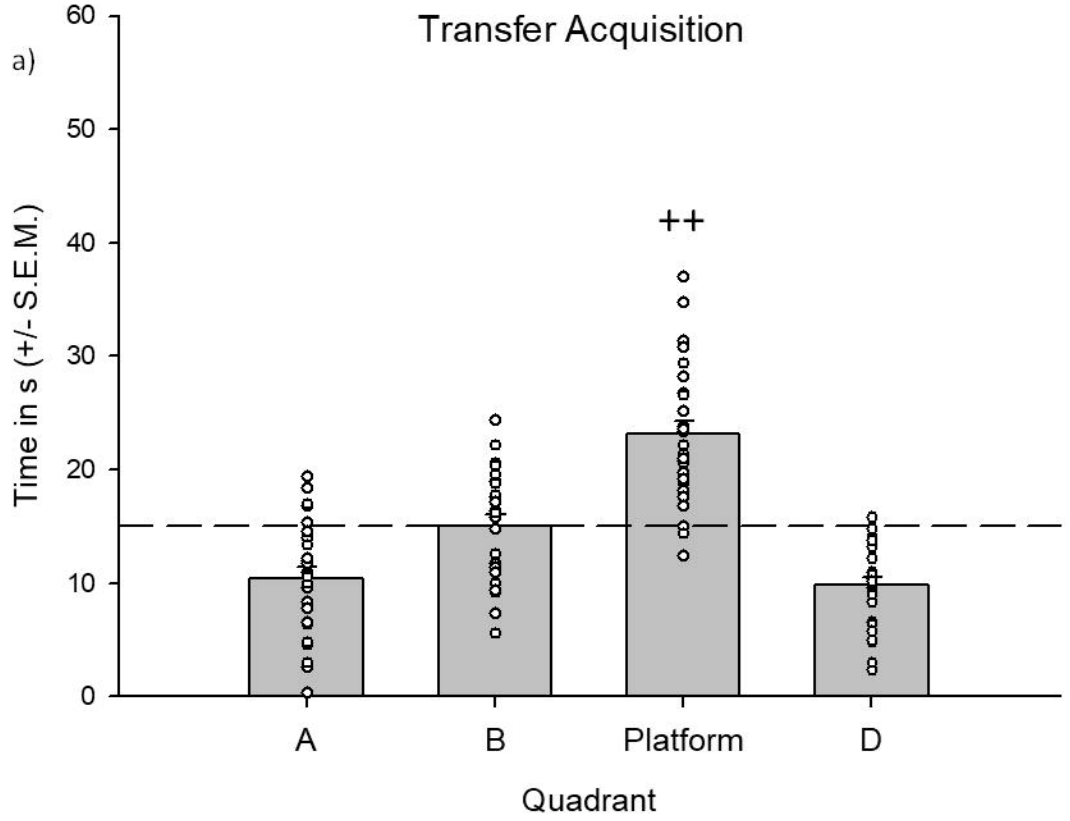
a)
Transfer Acquisition
Time in s (+/- S.E.M.)
60
50
40
30
20
10
0
++
A
B
Platform
D
Quadrant

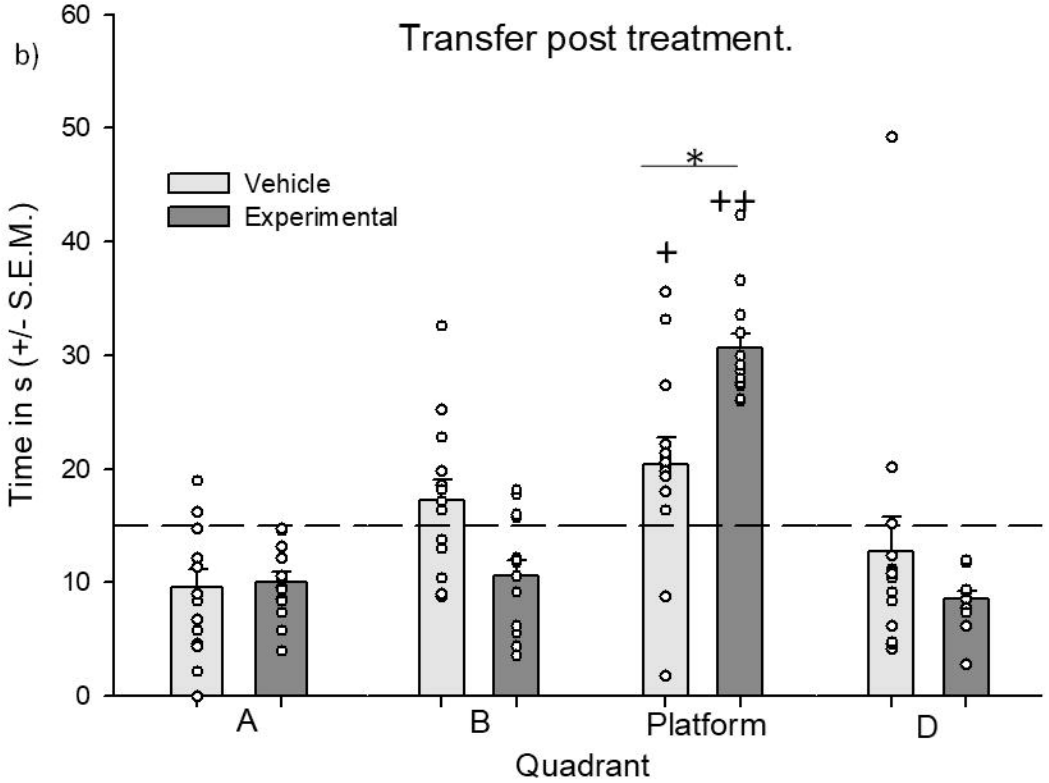
b)
Transfer post treatment.
Time in s (+/- S.E.M.)
Vehicle
Experimental
60
50
40
30
20
10
0
*
+
++
A
B
Platform
D
Quadrant

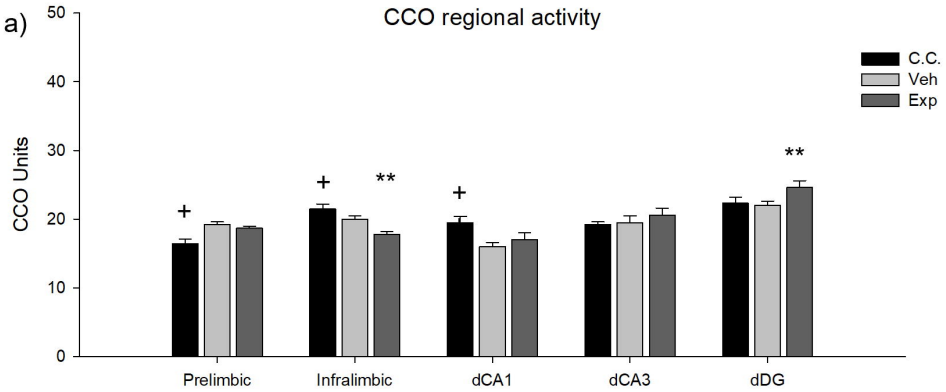
a)
CCO regional activity
C.C.
Veh
Exp
CCO Units
50
40
30
20
10
0
+
+
+
**
**
Prelimbic
Infralimbic
dCA1
dCA3
dDG

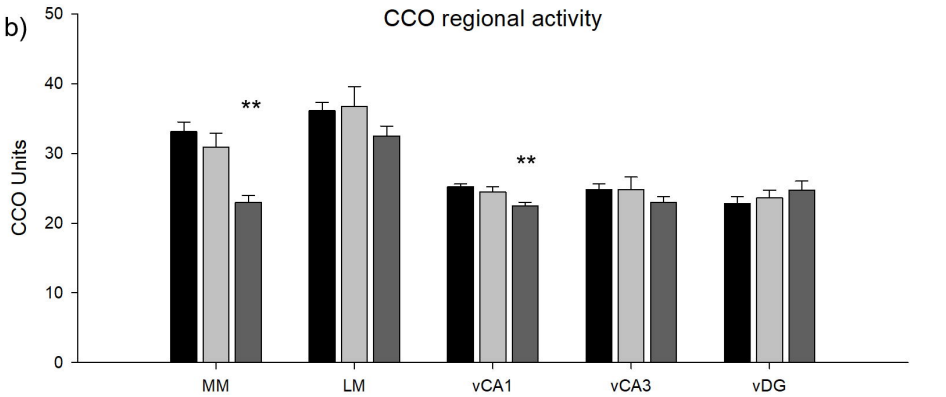
b)
CCO regional activity
CCO Units
50
40
30
20
10
0
**
**
MM
LM
vCA1
vCA3
vDG

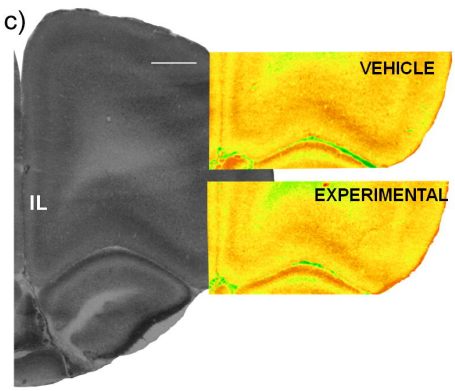
c)
VEHICLE
EXPERIMENTAL
IL

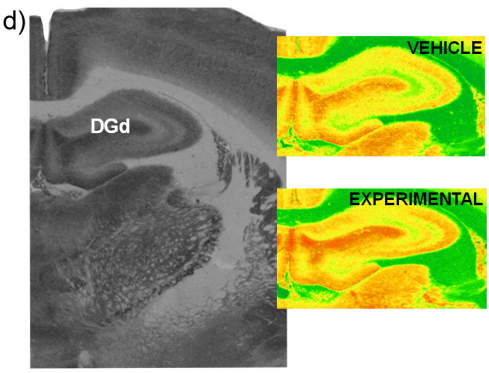
d)
VEHICLE
EXPERIMENTAL
DGd

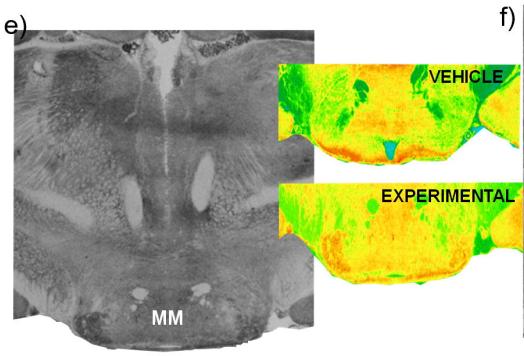
e)
VEHICLE
EXPERIMENTAL
MM

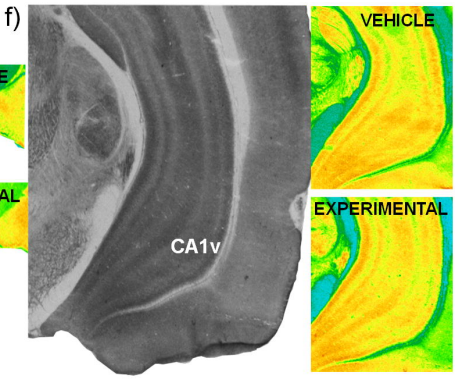
f)
VEHICLE
EXPERIMENTAL
CA1v

Table 1. Regional brain cytochrome c oxidase activity values. Mean ± S.E.M is shown for each experimental group. *(p<0.01) control cage vs experimental and Vehicle groups; ** (p<0.05) experimental *vs* control and saline groups; $^{+}$(p<0.01) control cage *vs* experimental group and $^{++}$(p<0.05) control *vs* vehicle group.

	n	Vehicle	n	EXP	n	C. Cage
CORTEX						
Prelimbic	8	19.2±0.4	6	18.7±0.3	8	16.4±0.7*
Infralimbic	8	20.0±0.5	6	**17.8±0.4****	8	21.5±0.7^{+}
Cingulate	8	19.8±0.7	6	19.2±0.5	8	21.2±0.9
Motor	8	20.6±0.4	6	19.9±0.3	8	20.5±0.4
Parietal	8	18.8±0.2	6	17.8±0.6	8	21.5±0.7^{+}
HIPPOCAMPUS						
CA1 dorsal	8	16.0±0.6	6	17.0±1.0	7	19.5±0.9^{++}
CA3 dorsal	8	19.5±1.0	6	20.6±1.0	7	19.2±0.4
DG dorsal	8	22.0±0.6	6	**24.6±1.0****	7	22.3±0.9
CA1 ventral	8	24.5±0.7	6	**22.5±0.5****	8	25.2±0.4
CA3 ventral	7	24.8±1.8	6	23.0±0.8	7	24.8±0.8
DG ventral	8	23.6±1.1	6	24.7±1.3	7	22.8±1.0
DIENCEPHALON						
Medial Mammillary Nuclei	6	30.9±2.0	6	**23.0±1.0****	6	33.1±1.4
Lateral Mammillary Nucleus	6	36.7±2.9	6	32.5±1.4	6	36.1±1.2
AMYGDALOID COMPLEX						
Basolateral Nucleus	7	21.7±0.8	6	21.1±1.6	7	20.6±0.9
Medial Nucleus	7	15.7±0.8	6	15.3±0.8	6	17.5±1.3
Central Nucleus	7	16.7±1.0	6	16.6±1.1	7	22.7±0.8*
Lateral Nucleus	7	16.7±0.9	6	14.8±6.6	7	19.5±1.6^{+}

EXP: Experimental group. C. Cage: Control Cage group. Vehicle: Vehicle group.